International Journal of
Molecular Microbiology

Research Article 2026 | Volume 9 | Issue 1 | 17-35

Open Access

Article Information

Received: January 7, 2026

Accepted: January 19, 2026

Published: January 25, 2026

Keywords

POEMS syndrome,
plasma cell dyscrasia,
cytokine signaling,
angiogenesis,
immune dysregulation.

Authors' Contribution

HT, MS, AHA, MF, AF, RF, NG, and KR jointly conceived the study and contributed equally to its design, analysis, and manuscript preparation. All authors approved the final version.

How to cite

Tariq, H., Saleem, M., Ali, A.H., Fatima, M., Fatima, A., Shahbaz, R.F., Gulzar, N., Ramzan, K., 2026. Integrative Computational Approaches to Protein Structure and Drug Design in POEMS Syndrome. Int. J. Mol. Microbiol., 9(1): 17-35.

***Correspondence**

Hamna Tariq
Email: hamna.tariq@uo.edu.pk

Integrative Computational Approaches to Protein Structure and Drug Design in POEMS Syndrome

Hamna Tariq[1]*, Muhammad Saleem[1], Ali Haider Ali[2], Mobeen Fatima[1], Aliza Fatima[1], Rida Fatima Shahbaz[1], Nimra Gulzar[1], Kainat Ramzan[3]

[1]Department of Molecular Biology, Faculty of Life Sciences, University of Okara, 53600, Punjab, Pakistan.
[2]Department of Biotechnology, Faculty of Life Sciences, University of Okara, 53600, Punjab, Pakistan.
[3]Department of Biochemistry, Faculty of Life Sciences, University of Okara, 53600, Punjab, Pakistan.

Abstract:

POEMS syndrome is a rare multisystem disorder associated with plasma cell dyscrasia, characterized by neurological, endocrine, hematological, and dermatological symptoms. Although the clinical features are well recognized, the underlying molecular mechanisms remain unclear. Current evidence suggests that abnormal cytokine signaling, immune dysregulation, and altered plasma cell function play key roles in disease development. In this study, we examined the molecular characteristics and interaction profiles of EHD1, STAT3, KLHL6, and LTB proteins involved in POEMS syndrome and explored potential therapeutic candidates using computational methods. Protein sequences were obtained from public databases and analyzed with protein–protein interaction and functional gene network tools, including STRING, HuRI, and GeneMANIA. The three-dimensional structures of these proteins were modeled through homology modeling and validated with standard structural assessment techniques. Molecular docking was performed with a selected set of FDA-approved drugs to assess potential protein–ligand interactions, with binding modes analyzed via molecular visualization software. Interaction network analysis revealed that EHD1 primarily functions in vesicular trafficking and endocytic recycling, while STAT3 serves as a central mediator of cytokine signaling. Additionally, KLHL6 is associated with plasma cell regulation and metabolic processes, and LTB is involved in immune and inflammatory pathways. Structural validation confirmed that the modeled proteins were suitable for docking studies. Several FDA-approved drugs, including Dasatinib, Simvastatin, Celecoxib, Niclosamide, Acitretin, and Cholesterol, exhibited favorable docking scores with the target proteins, indicating potential multi-target interactions. Overall, this computational work offers insights into the molecular networks and structural features linked to POEMS syndrome and identifies candidate compounds for future experimental testing. While the results are based on in silico analyses, they provide a foundation for future research aimed at better understanding and treating POEMS disorder.

Scan QR code to visit this journal.

INTRODUCTION

POEMS syndrome (peripheral neuropathy, organomegaly, endocrinopathy, monoclonal plasma cell proliferative disorder, and skin changes) is a rare paraneoplastic disorder that arises from the clonal proliferation of plasma cells in the bone marrow and is characterized by a constellation of multisystem features (Haider *et al.*, 2023). POEMS, also known as Crow–Fukase, Takatsuki syndrome, osteosclerotic myeloma, or PEP syndrome, the condition remains uncommon worldwide. Clinically, patients typically develop a progressive, predominantly motor neuropathy that leads to significant functional impairment (Dispenzieri and Buadi, 2013; Nozza, 2017). Additional manifestations, such as sclerotic bone lesions, papilledema, edema, ascites, serous effusions, thrombocytosis, erythrocytosis, pulmonary hypertension, thromboembolic events, and a frequent association with Castleman disease, reflect the systemic nature of the disease. The disorder is potentially life-threatening because complications, including capillary leak, multiorgan dysfunction, restrictive lung disease, and worsening disability, can occur (Dispenzieri, 2021; Suichi *et al.*, 2018).

Furthermore, POEMS appears to be driven mainly by immune and cytokine dysregulation, particularly elevated levels of VEGF, IL-1β, and IL-6, which promote angiogenesis, vascular permeability, and inflammation (Nozza, 2017; Tomasso *et al.*, 2022; Watanabe *et al.*, 1996). Recent genetic studies aimed at clarifying the biology of POEMS syndrome revealed widespread acquired mutations. Whole-exome sequencing identified 308 somatic mutations across 285 genes, and targeted sequencing detected 20 additional mutations in seven genes that were repeatedly altered such as KLHL6, LTB, EHD1, EML4, HELPHL1, HIPK1, and PCDH10 (Chen *et al.*, 2021; Kim, 2022; Nagao *et al.*, 2019)**.** Moreover, kelch-like family member 6 *(*KLHL6) is located on human chromosome 3q27.1 (~183,487,551–183,555,706 on GRCh38) and has an N-terminal BTB/POZ domain**,** a BTB and C-terminal Kelch (BACK) domain**,** and six Kelch repeat domains at the C-terminus, forming a scaffold that mediates, protein–protein interactions, that supports B-cell receptor signaling and plasma-cell differentiation. Alterations in KLHL6 can disrupt normal B-cell maturation and may promote the survival of abnormal plasma-cell clones, a process relevant to the development of POEMS syndrome (Bertocci *et al.*, 2017; Dhanoa *et al.*, 2013; Nagao *et al.*, 2019).

Additionally, Lymphotoxin-β (LTB) is encoded by the LTB gene on chromosome 12p13.31 (~6,307,142–6,310,943 on GRCh38). It is a member of the TNF superfamily and forms extracellular heterotrimers**.** Dysregulation of LTB can alter lymphoid tissue architecture**,** enhance inflammatory signaling**,** and increase cytokine release, contributing to immune abnormalities in POEMS syndrome (Upadhyay and Fu, 2013; Upadhyay and Fu, 2014). EHD1 is located on human chromosome 11q13.1 (about 69,841,532–69,880,431 on GRCh38) and encodes a protein with an ATP-binding G-domain and EH (Eps15 homology) domains that regulate the endocytic recycling of membrane receptors. Mutations in EHD1 can disrupt receptor trafficking and prolong cytokine and growth-factor signaling (Chakrabarti *et al.*, 2021; Jones *et al.*, 2020). STAT3, mapped on chromosome 17q21.31 (approximately 40,872,847–40,923,528 on GRCh38), contains coiled-coil, DNA-binding, SH2, and transactivation domains, and its activation promotes transcription of genes involved in plasma-cell survival and VEGF up-regulation (Kuchipudi, 2015; Samad *et al.*, 2025).

The structural and functional characteristics of EHD1 and STAT3 support their roles in signaling integration, receptor regulation, and immune activation, which help explain how their alterations contribute to the cytokine-rich, angiogenic, and inflammatory environment characteristic of POEMS syndrome. This study uses computational methods to examine molecular interactions between target proteins and potential ligands. Protein sequences will be retrieved from public databases, and interaction networks will be analyzed using STRING and related bioinformatics tools. Protein structures will be modeled through homology modeling, and candidate ligands will be selected from

online chemical libraries. Finally, protein–ligand complexes will be predicted and evaluated using in silico molecular docking tools to characterize binding affinity and interaction patterns, thereby supporting the identification of promising molecules for further investigation.

MATERIALS AND METHODS

Data Collection

Reference amino acid sequences for EHD1, STAT3, KLHL6, and LTB were obtained from the National Center for Biotechnology Information (https://www.ncbi.nlm.nih.gov) and the UniProt Knowledgebase (https://www.uniprot.org). All sequences were downloaded in FASTA format and used for downstream computational analyses. The overall study workflow is illustrated in **Fig. 1**.

Interaction Network Analysis

Protein–protein interaction networks were examined using STRING (v11.5, https://string-db.org), which integrates experimentally validated interactions, curated pathways, predictions, and literature-based evidence. The analysis focused on EHD1, STAT3, KLHL6, and LTB to map interacting partners and explore functional relationships. High-confidence interaction data from the Human Reference Interactome (HuRI, https://interactome-atlas.org) and functional predictions from GeneMANIA (http://www.genemania.org) further highlighted co-expression, physical interactions, and shared pathways (Bilal *et al.*, 2025b; Rasheed *et al.*, 2025).

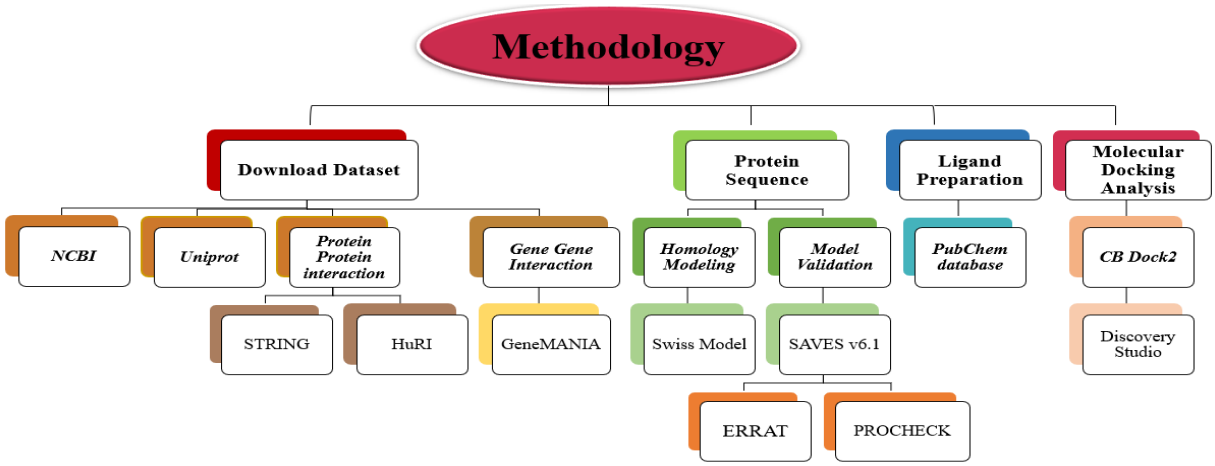

Fig. 1. Overall methodology of the present study.

Conformational Evaluation

The three-dimensional structures of EHD1, STAT3, KLHL6, and LTB were predicted using the SWISS-MODEL server (https://swissmodel.expasy.org), an automated platform for homology modeling. The FASTA sequences of each protein were submitted to identify appropriate template structures and construct accurate 3D models (Noman *et al.*, 2025; Sardar *et al.*, 2025).

Template Validation and Quality Assessment

The stereochemical quality and reliability of the predicted protein models were evaluated using the Structural Analysis and Verification Server (SAVES) (https://saves.mbi.ucla.edu). Model validation was performed using PROCHECK,

VERIFY3D, and ERRAT modules. ERRAT was used to evaluate non-bonded atomic interactions, while PROCHECK generated Ramachandran plots to analyze backbone dihedral angles (φ and ψ). Protein models with more than 90% of residues in the most favored regions of the Ramachandran plot were considered structurally acceptable (BILAL *et al.*, 2025a; Ramzan and Noman, 2024).

Ligand Selection

A total of 15 ligands were selected, and their structures in SDF format were retrieved from the PubChem database (https://pubchem.ncbi.nlm.nih.gov). Literature was reviewed to assess the biological and pharmacological properties of these compounds, and the ligand structures were prepared in suitable formats for docking analysis (Bilal *et al.*, 2025b; Noman *et al.*, 2025).

Virtual Drug Designing and Screening

Protein–ligand docking was carried out using CB-Dock2 (http://183.56.231.194:8001/cb-dock2/index.php), a blind docking server optimized for cavity detection and binding pose prediction. The platform uses an automated workflow and shows strong performance in identifying likely binding orientations (Liu *et al.*, 2022). Docking outputs were visualized in Discovery Studio Visualizer (https://discover.3ds.com/discovery-studio-visualizer-download), where 2D and 3D interaction profiles were examined to assess hydrogen bonding, hydrophobic contacts, and binding conformations contributing to ligand stability within the active site (Bilal *et al.*, 2025b; Sardar *et al.*, 2025).

RESULTS

Download data

The reference sequences of the selected proteins were retrieved from UniProt (Table 1). These reference sequences were used for all subsequent computational analyses.

PPI Interaction Analysis

Protein–protein interaction (PPI) network analysis revealed distinct interaction topologies among the investigated proteins, highlighting their differential contributions to disease-associated cellular processes. The EHD1 interaction network predicted by the STRING server includes RBSN, MICALL1, RAB11FIP2, SNAP29, RAB11FIP5, RAB11FIP1, PACSIN2, RAB8A, VPS45, RAB5A family members, indicating involvement in vesicle trafficking and endocytic recycling (Figure 2A). Moreover, STAT3 is positioned within a densely connected network containing EGFR, JAK1, JAK2, JAK3, STAT1, STAT5A, STAT5B, SRC, EP300, and PIAS3, consistent with JAK–STAT signaling and transcriptional regulation (Figure 2B). The KLHL6 network exhibits limited connectivity and comprises GLUL, GAD1, GLUD1, CTBP2, COPS8, and GPRL1, indicating an association with metabolic and homeostatic processes (Figure 2C). The LTB network comprises immune-related genes, including LTA, TNFRSF13C, TNFRSF1B, CD40LG, RELB, TRAF3, and LST1, which reflect their involvement in TNF-related and NF-κB signaling pathways. Nodes represent proteins and edges indicate known or predicted interactions (Figure 2D).

Table 1. Reference protein information.

Protein	Full Name	UniProt ID	Length (aa)
EHD1	EH domain-containing protein 1	Q9H4M9	Varies by isoform
STAT3	Signal Transducer and Activator of Transcription 3	P40763	~770
KLHL6	Kelch-like protein 6	Q8WZ60	~600
LTB	Lymphotoxin-beta	Q06643	244

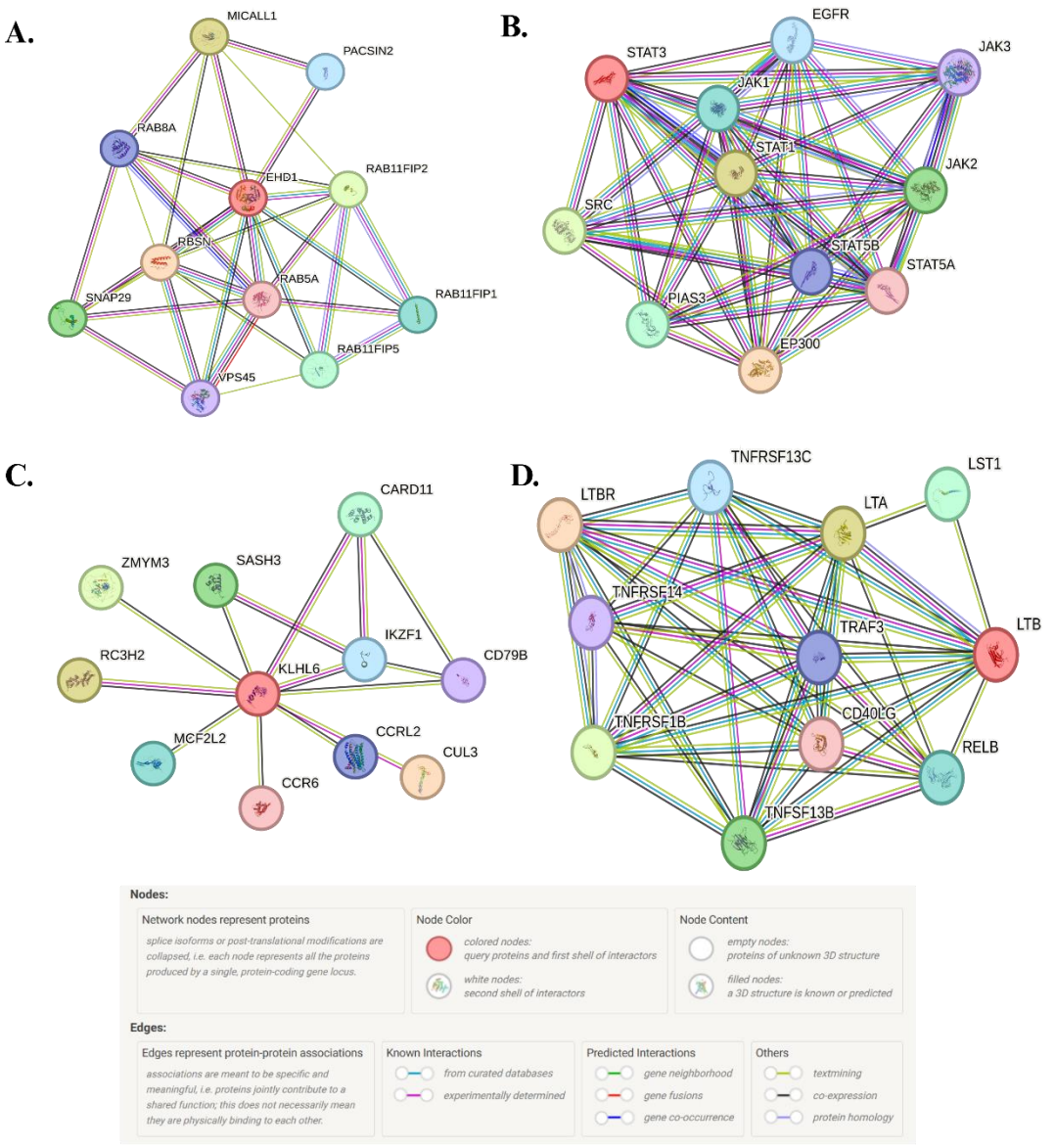

Fig. 2(A-D). Protein–protein interaction networks generated using the STRING database.

From HuRI analysis, the EHD1 formed a compact and highly interconnected module, directly linking EHD1 with EHD3, RAB11FIP2, RBSN, SNAP29, MICAL1, ANKFY1, and HSPB1**.** This tightly organized interaction cluster underscores the critical involvement of EHD1 in endocytic recycling and membrane trafficking**,** processes frequently implicated in disorders associated with altered intracellular transport and cellular homeostasis (Figure 3A). In contrast, STAT3 exhibited a highly dense and expansive interaction network**,** engaging numerous signaling and regulatory proteins. This extensive connectivity is consistent with STAT3's established role as a central signaling hub**,** integrating inflammatory, proliferative, and transcriptional pathways commonly dysregulated in human diseases (Figure 3B).

The KLHL6 interaction network identified PPP1R1B, FH, CRY2, BYSL, TMPO, and SBDS, which are potentially associated with protein quality control, metabolic regulation, and cellular stress responses, and may contribute to disease susceptibility under specific

physiological or pathological conditions (Figure 3C). Notably, the TNAGL-centered network positioned TNAGL as a prominent interaction hub, linking with KRTAP2-2, KRTAP2-4, NOTCH2NL, BAG4, TRIP13, RBPMS, NBPF19, PITX2, MDFI, and PROP1 (Figure 3D). The functional heterogeneity of these interactors implicates TNAGL in transcriptional regulation, developmental signaling, and structural organization**,** suggesting a potential role in disease mechanisms involving altered gene regulation and cellular differentiation. Such network heterogeneity provides mechanistic insights into protein function and highlights potential molecular pathways contributing to POEM disease development and progression.

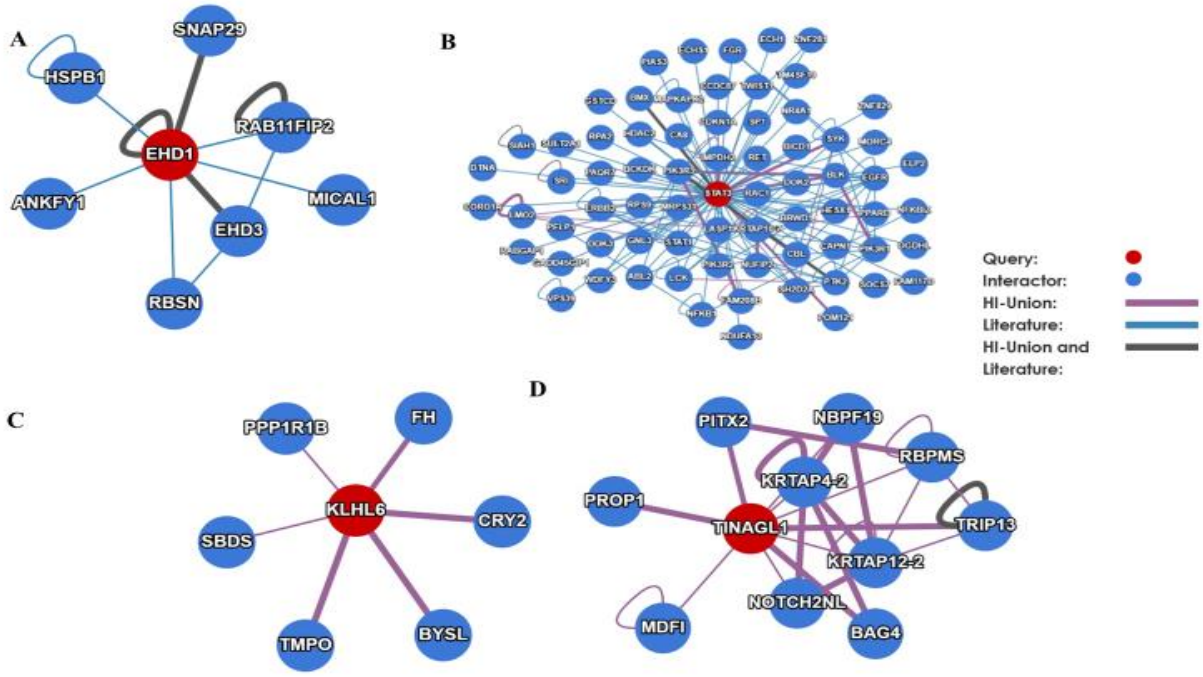

Fig. 3(A-D). Protein–protein interaction networks of EHD1, STAT3, KLHL6, and TNAGL.

Functional gene–gene interaction networks

Gene–gene interaction networks were constructed using GeneMANIA by integrating physical interactions, co-expression, predicted functional associations, co-localization, genetic interactions, pathway enrichment, and shared protein domains. As shown in (Figure 4A), the EHD1-centered network displayed strong functional associations with EHD3, EHD4, RIN3, RBSN, VPS45, IGF1R, AKR1B1, FADD, SNAP29, and OPA1**,** highlighting its role in vesicle transport and intracellular membrane dynamics. In Figure (4B), STAT3 showed prominent interactions with STAT1, STAT5B, IL6ST, IL6R, PIAS3, EGFR, CRP, CTR9, PIPN2, PRKCD, PDIA3, and PTPRT**,** consistent with its function as a central regulator of immune signaling, transcriptional control, and disease-associated signal transduction. The KLHL6 network (Figure 4C) exhibited interacting partners, including KLHL7, IL21R, EAF2, KBTBD8, GGA2, LAMTOR5, FCRL4, MMP12, and NUDCD3**,** suggesting a context-dependent regulatory role**,** particularly in immune-related and intracellular trafficking processes. As illustrated in Figure 4D, LTB displayed strong connections with LTBR, TNF, ETS1, MMRN2, MADD, TRAF3IP3, FASLG, TNFSF14, CCR7, and LTA**,** indicating a central role in immune regulation and inflammatory response pathways.

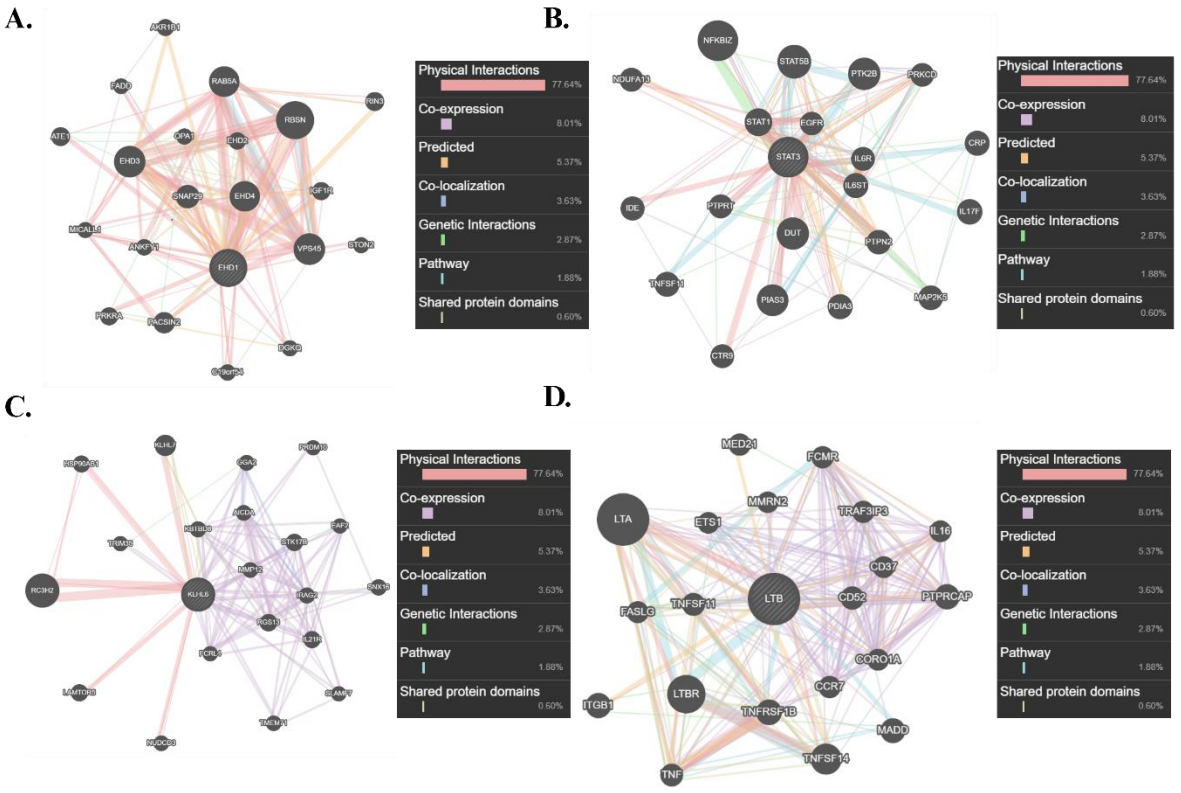

Fig. 4(A-D). GeneMANIA-based functional interaction networks of EHD1, STAT3, KLHL6, and LTB.

Structure Modeling and Validation

The 3D structures of EHD1, STAT3, TNFC/LTB, and KLHL6 were retrieved from the Swiss Model database and evaluated for reliability before further analysis. EHD1_MOUSE (534 amino acids, UniProt ID: Q9WVK4.1.A) was modeled as a monomer, reflecting its predicted oligomeric state. The model showed a high confidence score of 0.90 and covered 99.44% of the protein sequence. Structural validation identified Model 2 as the most accurate, with an ERRAT score of 95.63%. Ramachandran analysis revealed that 92.70% of residues fell within the most favored regions, confirming excellent stereochemical quality. PROCHECK results further supported the reliability of this model (Figure 5A). STAT3_MOUSE (770 amino acids, UniProt ID: P42227.1.A) was similarly modeled as a monomer. The model achieved a confidence score of 0.85 and spanned 99.87% of the sequence. Validation revealed an ERRAT score of 94.20%, with 89.90% of residues in the most favored regions according to Ramachandran analysis. PROCHECK analysis confirmed the structure's accuracy and suitability for downstream studies (Figure 5B).

In addition, TNFC_MARMO (244 amino acids, UniProt ID: Q9JM10.1.A) was retrieved and modeled as a monomer. The model showed a confidence score of 0.78, covering 85.25% of the sequence. ERRAT validation yielded a score of 79.70%, and Ramachandran analysis indicated that 88.60% of residues occupied the most favored regions, demonstrating reasonable structural reliability. PROCHECK analysis confirmed the overall quality of the predicted structure (Figure 5C). KLHL6_HUMAN (621 amino acids, UniProt ID: Q8WZ60.1.A) was modeled as a monomer, with the model achieving a confidence score of 0.88 and covering 100% of the sequence. Validation using ERRAT gave a score of 87.90%, and Ramachandran analysis showed that 83.10% of residues were in the most favored regions.

PROCHECK analysis further supported the model's accuracy (Figure 5D). However, these results confirm that all four protein models are structurally reliable and suitable for subsequent molecular docking and interaction studies.

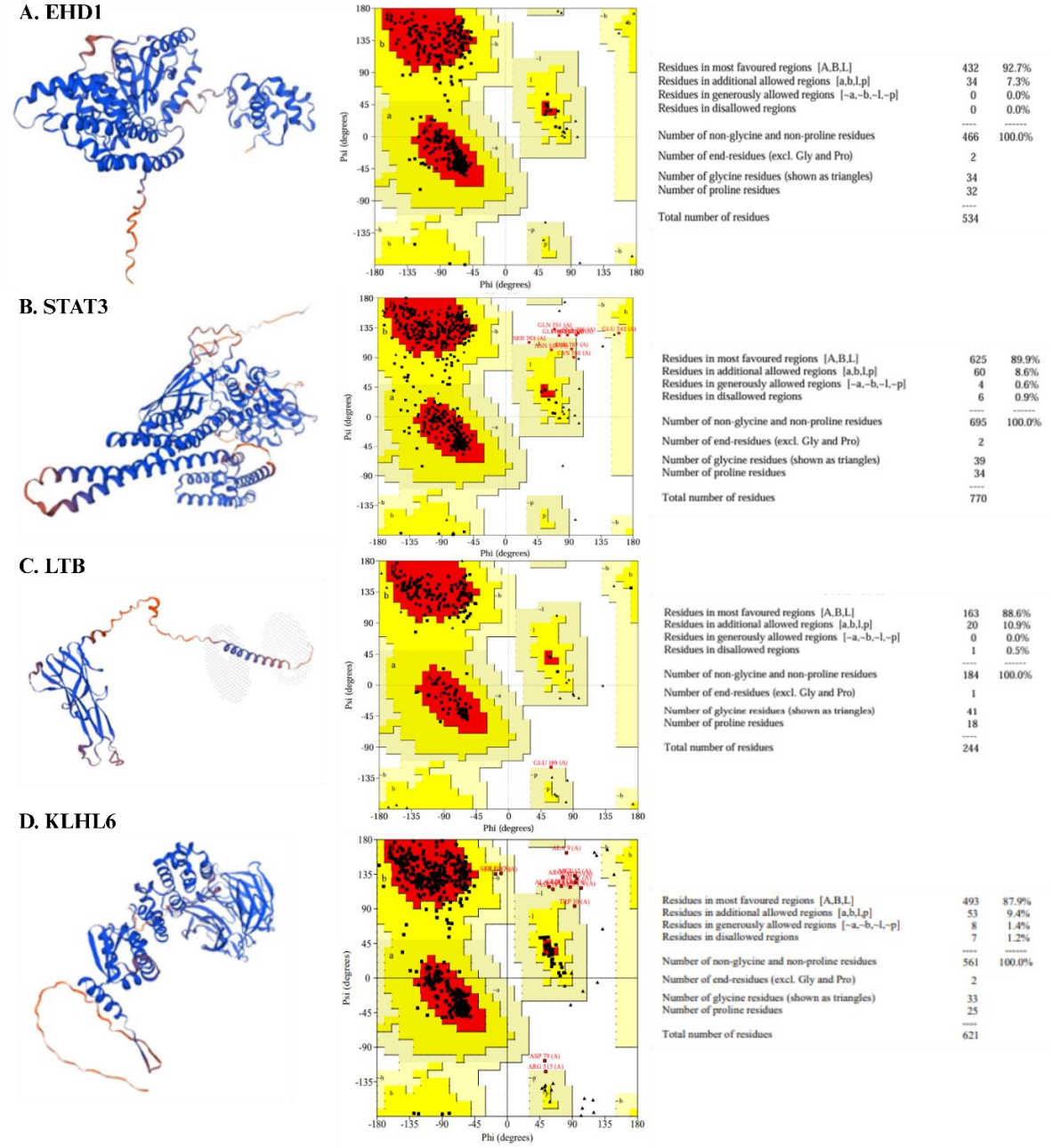

Fig. 5(A-D). Predicted 3D structures of **(A)** EHD1 **(B)** STAT3 **(C)** TNFC and **(D)** KLHL6 (blue: α-helices and β-sheets; orange: unstructured regions). Ramachandran plots show residues in favored (red), allowed (yellow), generously allowed (light yellow), and disallowed (white) regions. Validation statistics on the right confirm the stereochemical quality and reliability of each model.

Virtual Screening of Docking Compounds

Based on the docking scores of FDA-approved compounds against EHD1, STAT3, KLHL6, and LTB, the top candidates with the strongest predicted binding across multiple targets for POEM disorder are Celecoxib, Simvastatin, Dasatinib, Acitretin, Niclosamide, and Cholesterol (Table 2). Among the compounds analyzed, Celecoxib, Simvastatin, and Dasatinib showed the strongest predicted binding affinities with EHD1 and KLHL6, suggesting their potential to modulate key molecular pathways involved in POEM disorder. Niclosamide and Cholesterol also displayed notable binding across multiple targets, while Acitretin and Amoxicillin exhibited moderate interactions. The docking analysis revealed that the tested ligands established diverse networks of stabilizing interactions within the binding pockets of the target proteins (Table 3).

Table 2. Docking scores of FDA-approved compounds against target proteins.

Compound	Molecular Formula	Molecular Weight (g/mol)	EHD1 (kcal/mol)	STAT3 (kcal/mol)	KLHL6 (kcal/mol)	LTB (kcal/mol)
Cholesterol	$C_{27}H_{46}O$	386.65	-8.7	-7.1	-10.5	-6.8
Abacavir	$C_{14}H_{19}N_6O$	286.35	-7.7	-6.7	-8.2	-6.1
Rituximab	Protein	~145,000	-7.4	-5.8	-7.1	-5.2
Acitretin	$C_{21}H_{26}O$	326.43	-8.8	-6.7	-9.0	-6.4
Celecoxib	$C_{17}H_{14}F_3N_3O_2$	381.37	-9.4	-7.2	-9.9	-7.1
Isoniazid	$C_6H_7N_3O$	137.14	-6.7	-5.3	-6.0	-4.9
Simvastatin	$C_{25}H_{38}O_5$	418.57	-9.4	-7.4	-10.2	-6.9
Amoxicillin	$C_{16}H_{19}N_3O_5S$	365.40	-7.5	-6.6	-9.3	-6.1
Dasatinib	$C_{26}H_{26}ClN_7O$	488.01	-8.8	-7.9	-10.5	-7.9
Tyrosine	$C_9H_{11}NO_3$	181.19	-7.3	-5.5	-6.3	-5.1
Niclosamide	$C_{13}H_8Cl_2N_2O_4$	327.12	-9.2	-7.3	-9.5	-6.7

The EHD1 had the strongest interactions with Celecoxib and Simvastatin, both showing a docking score of -9.4 kcal/mol, followed closely by Niclosamide at -9.2 kcal/mol and Dasatinib and Acitretin at -8.8 kcal/mol. In Figure (6), Celecoxib formed several polar contacts, mainly involving ASN288, SER284, LEU63, VAL61, ILE214, and ALA179. The surrounding hydrophobic residues, such as ARG215, LEU187, PHE178, LEU285, and VAL182, contributed to the additional stabilization of the complex. Simvastatin similarly engaged EHD1 through hydrogen-bonding interactions with residues including GLU180, ARG181, ASN288, and ASP281, accompanied by hydrophobic contacts with MET60, PHE178, and LEU285, suggesting a favorable accommodation within the binding cavity. Niclosamide primarily interacted through polar residues such as LYS213, ARG292, and TYR253, while hydrophobic residues such as LEU285 and ILE186 reinforced the ligand placement. Dasatinib and Acitretin showed mixed interaction patterns, combining multiple hydrogen bonds (GLU180, SER284, and ASP212) and strong hydrophobic contacts contributed by TRP177, PHE178, and LEU285, indicating comparatively tighter binding behavior within the pocket (Table 3).

Moreover, Dasatinib exhibited the strongest binding with a docking score of -7.9 kcal/mol, followed by Simvastatin (-7.4 kcal/mol) and Niclosamide (-7.3 kcal/mol). Celecoxib (-7.2 kcal/mol) and Cholesterol (-7.1 kcal/mol) also showed relatively strong interactions, suggesting potential effectiveness in modulating STAT3 activity. For STAT3, Celecoxib and Simvastatin exhibited notable hydrogen-bonding interactions with LYS244, CYS251, GLY254, and THR133, while hydrophobic residues, including TRP243, ILE249, PRO255, and TRP510, provided additional stabilization. Cholesterol formed hydrogen bonds with GLU506, GLU324, and ARG325, while hydrophobic contacts involving TRP243 and ILE258 indicated insertion into the hydrophobic core. Dasatinib and Niclosamide displayed strong polar interactions, particularly with CYS259, GLY254, and ASN257,

accompanied by hydrophobic contributions from TRP510, ILE249, and GLN247 (**Table 3**).

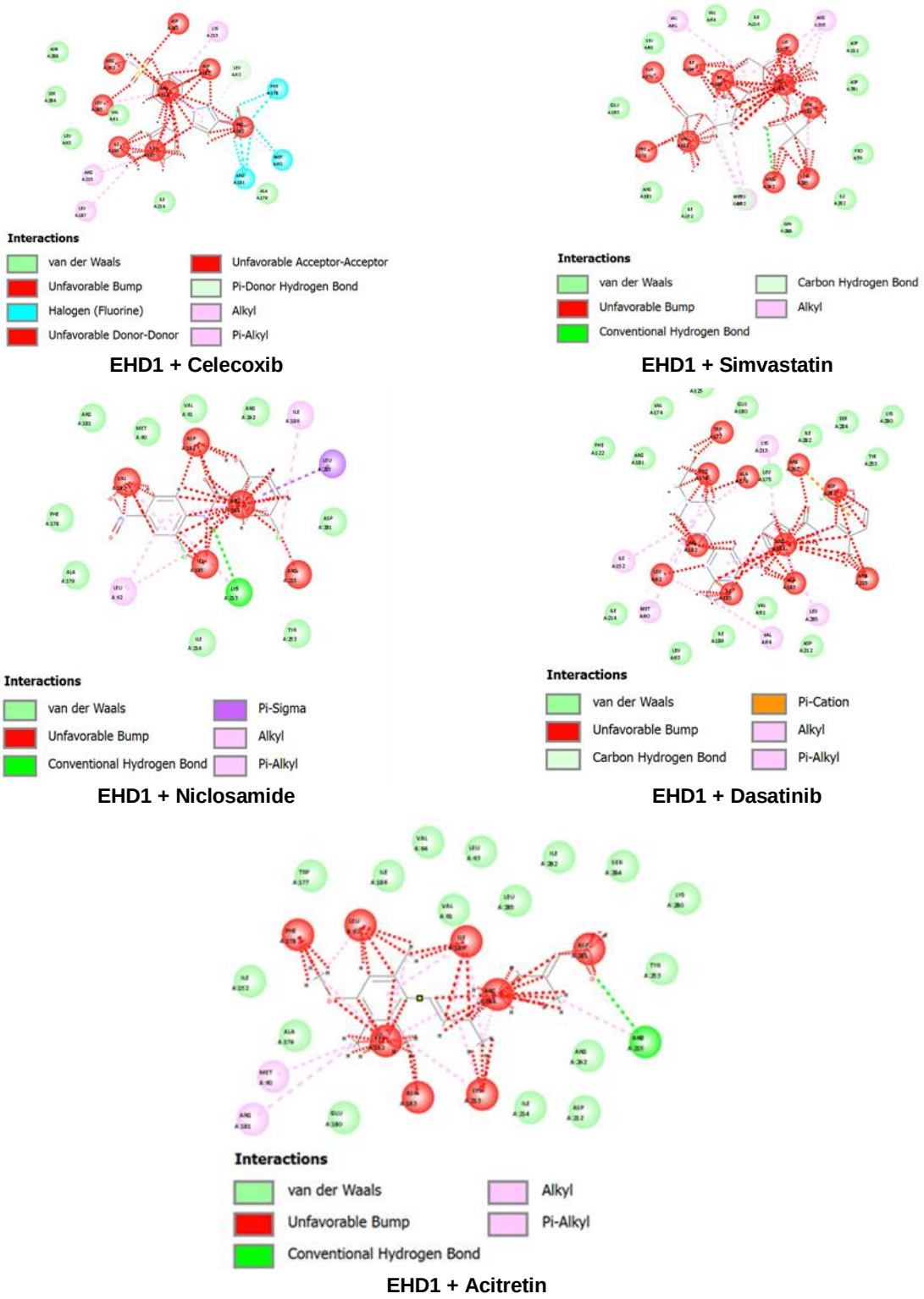

Fig. 6. Molecular docking poses between EHD1 and the ligands are visualized, highlighting key residues involved in ligand binding as predicted through docking studies using Discovery Studio.

Table 3. Interaction Profiles of Hydrophilic and Hydrophobic Residues in EHD1, STAT3, KLHL6, and LTB with Docked Ligands Using Discovery Studio.

Protein–Ligand	Hydrophilic interactions	Hydrophobic interactions
EHD1 – Celecoxib	ASN288, SER284, LEU63, VAL61, ILE214, ALA179, LEU62	ARG215, LEU187, LYS213, PHE178, MET60, ARG181, ASP281, ARG292, LEU285, ILE186, ILE185, ASP183, ARG184, VAL182
EHD1 – Simvastatin	VAL64, ILE214, LEU63, GLU180, ARG181, ILE152, ASN288, ILE282, PRO59, ASP281, ASP212, LEU62	VAL61, ARG215, MET60, ALA179, PHE178, VAL182, ILE186, ILE185, ARG184, ARG292, LEU285, ASP183, LYS213
EHD1 – Niclosamide	LYS213, ARG292, VAL61, MET60, ARG181, PHE178, ALA179, ILE214, TYR253, ASP281	LEU285, ILE186, LEU62, ARG215, ARG184, ILE185, ASP183, VAL182
EHD1 – Dasatinib	PHE122, ARG181, VAL174, LEU125, GLU180, LEU175, ILE282, SER284, TYR253, LYS280, ILE214, LEU63, ILE186, VAL61, ASP212	TRP177, PHE178, ALA179, ARG292, ASP281, ARG215, ARG184, ASP183, ILE185, VAL182, LEU62, LYS213, LEU285, VAL64, MET60, ILE152
EHD1 – Acitretin	ILE152, ALA179, GLU180, TRP177, ILE186, VAL61, VAL64, LEU63, LEU285, ILE282, SER284, ARG215, LYS280, TYR253, ARG292, ILE214, ASP212	MET60, ARG181, PHE178, LEU62, VAL182, ASP183, LYS213, ILE185, ARG184, ASP281
STAT3 – Celecoxib	TRP243, LYS244, CYS259, THR133, PRO132, TRP510, ASN481	CYS251, ILE252, PRO256, ILE258, ASN257, PRO255, GLN247, ARG246, ARG245, GLN248, ILE249, ALA250
STAT3 – Cholesterol	GLY254, GLU506, CYS251, ILE252, CYS259, LEU260, GLU324, ARG325, GLN326, LYS244, VAL323, ASP242, ARG245	TRP243, GLN247, ILE258, ARG246, ILE249, TRP510, ALA250, PRO255, ASN257
STAT3 – Dasatinib	ARG350, CYS259, PRO256, PRO255, GLY254, ALA250, ASN257, ARG245, LEU459, LYS244	CYS251, ILE258, GLN248, GLN247, ARG246, LEU260, GLU324, TRP510, GLU506, ILE249, TRP243
STAT3 – Simvastatin	LYS244, CYS251, ILE252, ARG245, GLY253, GLY254, LEU260, CYS259, THR133, PRO132	TRP510, PRO256, PRO255, ASN257, ARG246, ILE258, ILE249, GLN248, ALA260, GLN247, TRP243
STAT3 – Niclosamide	PRO256, ASN257, CYS259, GLY254, LYS244, CYS251	TRP243, ILE252, PRO255, ILE258, GLN247, ARG246, ILE249, ARG245, ALA250, TRP510, GLN248
KLHL6 – Cholesterol	LEU560, THR603, CYS556, ARG559, SER318, LEU343, MET313, ASP225, GLN317, GLU315, LEU265, SER513, ARG515, SER306, GLU307, THR309	PRO555, ILE305, ASN558, GLU319, ASN557, PRO311, LYS310, ARG312, ARG262, PHE514
KLHL6 – Dasatinib	ASP226, HIS314, LEU343, GLU315, ASP225, CYS556, ARG262, ARG559, VAL512, ARG517, TYR519, ASN557, SER318, SER306, ARG605, LEU265, ARG308	MET313, ARG312, PRO311, PRO555, PHE514, SER513, LYS310, THR309, ASN558, ARG515, ILE305, LEU560, GLU319
KLHL6 – Simvastatin	TYR297, GLU307, ARG606, LEU265, SER306, ARG515, ASP225, ARG312, SER318, LEU343, LEU560, TYR561, ARG262	THR309, ILE306, PHE514, PRO311, LYS310, ASN558, ASN557, CYS556, GLU319, ARG559, PRO555
KLHL6 – Celecoxib	ARG262, LEU343, ARG308, GLU307, ILE304, ARG605, ARG559, PRO555, LEU560, ARG515	PRO311, SER306, LYS310, ASP225, THR309, GLU319, ASN557, CYS556, ASN558, PHE514, ILE305, TYR297
KLHL6 – Niclosamide	LEU343, CYS556, ARG559, ARG515, ARG262, ARG312, LEU265, THR309	PRO311, ASN557, ASN558, LYS310, PHE514, ILE305, SER306, PRO555, GLU319
LTB – Dasatinib	GLU180, SER161, SER162, GLU183, GLY181, GLY206, GLY208, PHE207, CYS137, TYR136, HIS91	LEU125, LEU92, LEU138, PHE237, VAL221, LEU179, ALA182, LEU135, VAL206, LEU163, ALA240, ALA90, PHE238, GLY239
LTB – Celecoxib	SER162, TYR134, GLY239, GLY208, GLY206, TYR136, CYS137, GLY181, SER161, GLU180	VAL139, VAL205, ALA182, LEU179, LEU163, LEU135, PHE237, PHE238, LEU138
LTB – Simvastatin	SER161, SER162, GLU180, GLY181, GLY206, GLY208	ALA182, PHE237, PHE238, GLY239, LEU135, LEU163, LEU179, VAL139, VAL205, LEU138, TYR136
LTB – Cholesterol	GLU183, GLY181, GLY209, GLY206, GLY208, CYS137, TYR136	VAL139, VAL221, ALA182, GLY239, TYR134, LEU135, LEU179, PHE237, LEU138, PHE238, LEU163, VAL205
LTB – Niclosamide	GLY208, GLY239, LEU163, TYR136, CYS137, GLY181, GLY206	PHE237, PHE238, LEU138, ALA182, LEU179, VAL205

This study highlights Dasatinib, Simvastatin, and Niclosamide as the most promising candidates for interacting with STAT3, which may contribute to therapeutic strategies for POEM disorder (Figure 7).

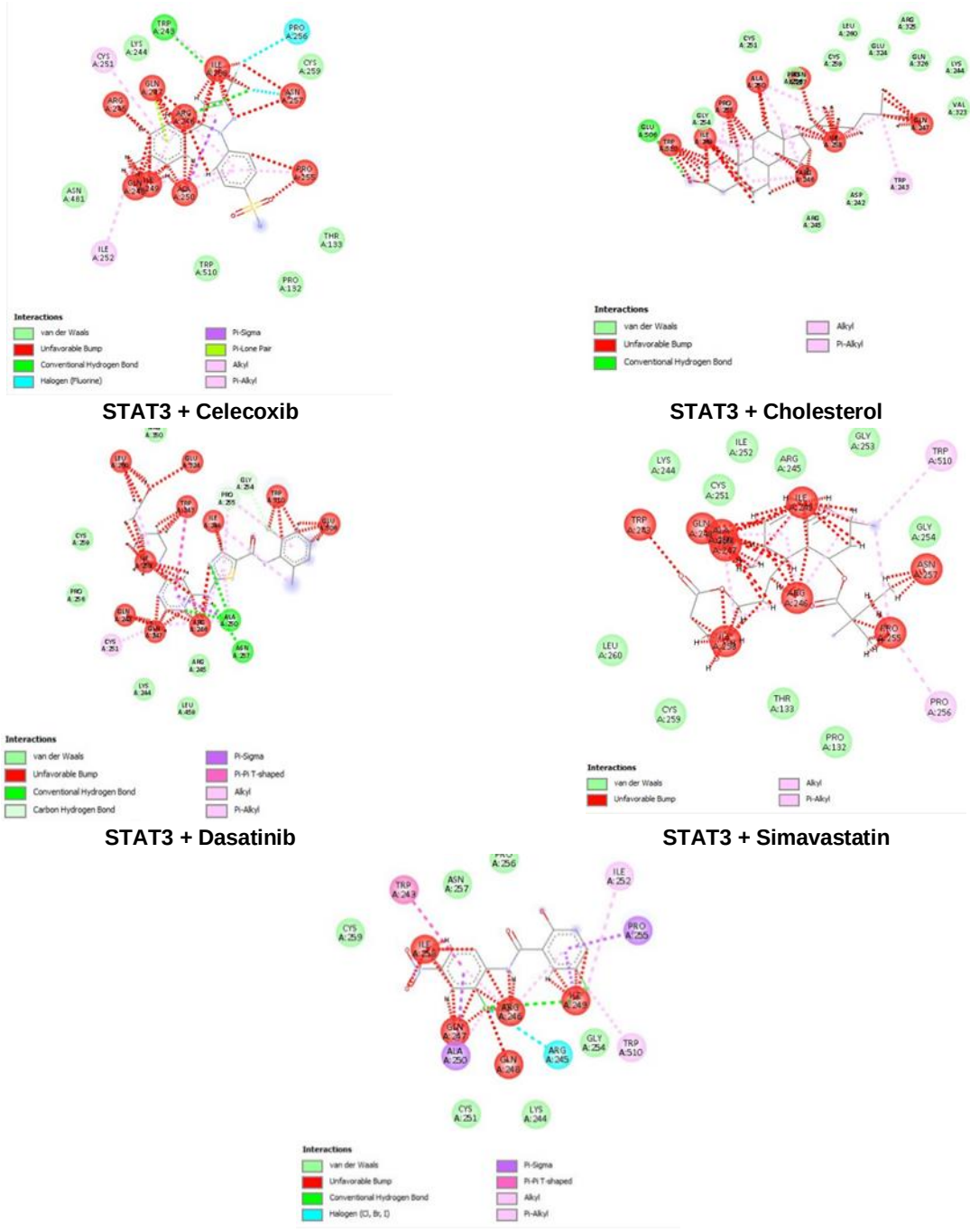

Fig. 7. Molecular Interactions of STAT3 with Selected Ligands Based on Molecular Docking Analysis in Discovery Studio.

Additionally, Cholesterol and Dasatinib demonstrated the strongest binding, each with a docking score of -10.5 kcal/mol, followed closely by Simvastatin (-10.2 kcal/mol) and Celecoxib (-9.9 kcal/mol). Niclosamide (-9.5 kcal/mol), Amoxicillin (-9.3 kcal/mol), and Acitretin (-9.0 kcal/mol) also showed relatively strong interactions with KLHL6. In **Table 3**, cholesterol and other ligands were stabilized through extensive hydrogen-bonding interactions with residues such as THR603, ARG559, GLU315, SER318, and ASP225. Surrounding hydrophobic

residues (PHE514, PRO555, LEU560, and ILE305) further supported ligand anchoring. Dasatinib and Simvastatin showed similar interaction modes, combining hydrogen bonding with ASP226, ARG262, SER318, and ARG515 while engaging hydrophobic regions defined by MET313, PHE514, and PRO311. Celecoxib and Niclosamide interacted primarily through polar residues, including ARG262, GLU307, THR309, and ARG515, supported by hydrophobic contacts provided by PRO311, PHE514, and LEU560 (Figure 8).

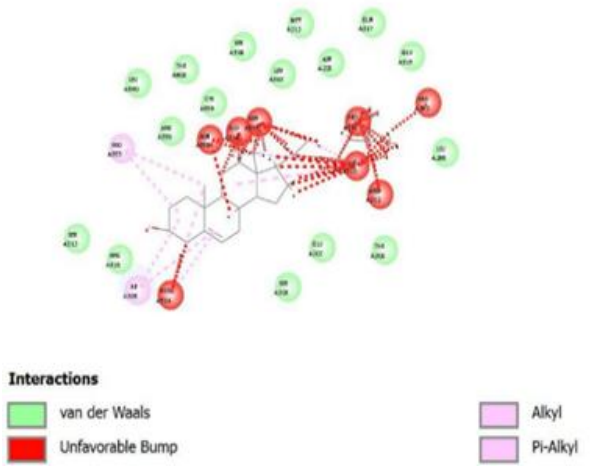

KLHL6 + Cholesterol

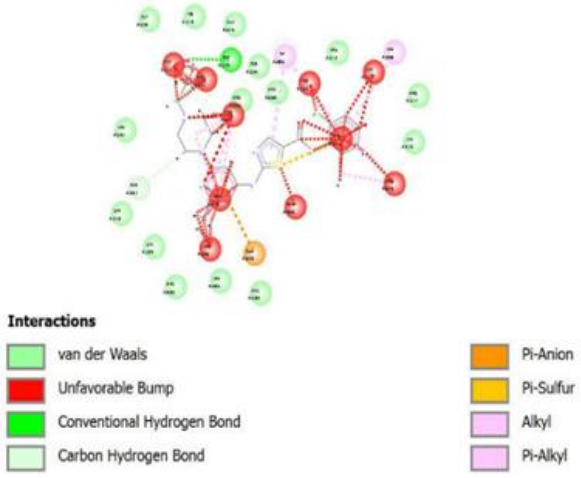

KLHL6 + Dasatinib

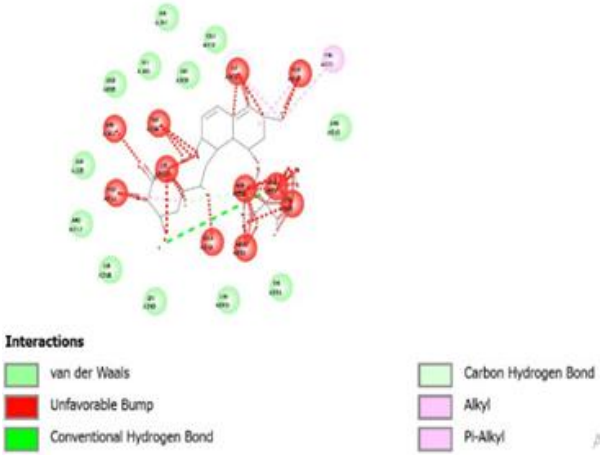

KLHL6 + Simvastatin

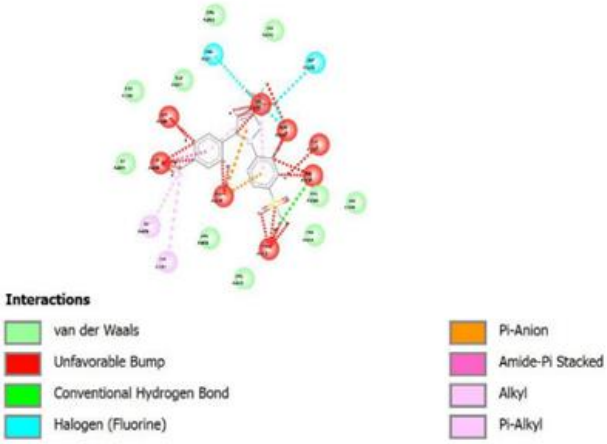

KLHL6 + Celecoxib

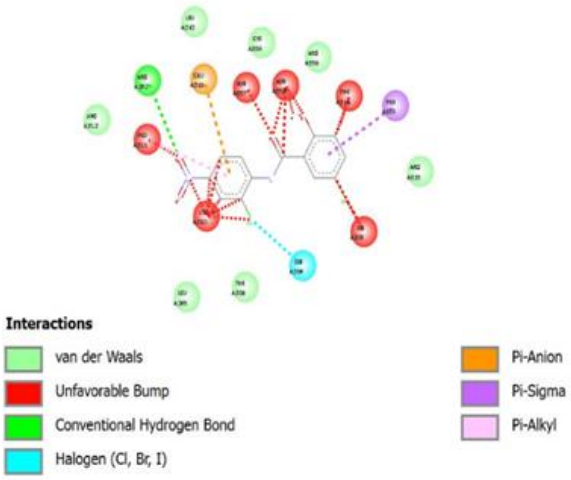

Fig. 8. Molecular Interactions of KLHL6 with Selected Ligands Based on Molecular Docking Analysis in Discovery Studio.

Moreover, the lowest docking energies were obtained for Dasatinib (−7.9 kcal/mol), followed by Celecoxib (−7.1 kcal/mol), Simvastatin (−6.9 kcal/mol), Cholesterol (−6.8 kcal/mol), and Niclosamide (−6.7 kcal/mol), indicating that these compounds exhibit comparatively stronger binding affinity toward LTB than the other screened ligands. Analysis of the docking interactions revealed that all ligands were stabilized within the LTB cavity through a combination of hydrogen-bonding and hydrophobic interactions (Table 3). Dasatinib formed key polar contacts with GLU180, SER161, SER162, GLU183, GLY181, GLY206, and GLY208, while hydrophobic stabilization was contributed by residues including LEU138, PHE237, LEU179, VAL206, and LEU163. Celecoxib interacted with SER162, TYR134, GLU180, GLY181, and GLY208, and was further stabilized by VAL139, LEU179, LEU163, and PHE238. Simvastatin formed hydrogen bonds with SER161, SER162, GLU180, GLY181, GLY206, and GLY208, with additional hydrophobic support from ALA182, PHE237, LEU135, and VAL205. Cholesterol predominantly engaged hydrophobic residues VAL139, LEU135, LEU179, PHE237, and VAL205, while maintaining limited polar contacts with GLU183, GLY181, and GLY208. Niclosamide mainly interacted with GLY208, GLY239, GLY206, and TYR136, accompanied by hydrophobic contacts with PHE237, PHE238, LEU138, and VAL205 (Figure 9).

The compounds identified in this study may serve as potential candidates for further investigation through laboratory experiments, including in vitro and in vivo assays, to determine their effectiveness against POEM disorder. The docking results offer insights that can support the design and optimization of drugs targeting multiple pathways. Combining these findings with pharmacokinetic and toxicity assessments could help in selecting the most promising compounds for future studies. However, the study is limited by its reliance on computational predictions, which may not fully reflect the dynamic behavior of proteins or the complexity of biological systems. Predicted binding strengths may differ from actual biological activity due to factors such as metabolism, bioavailability, and off-target interactions. Moreover, only a subset of FDA-approved compounds was analyzed, which could exclude other molecules with higher therapeutic potential, highlighting the importance of experimental validation.

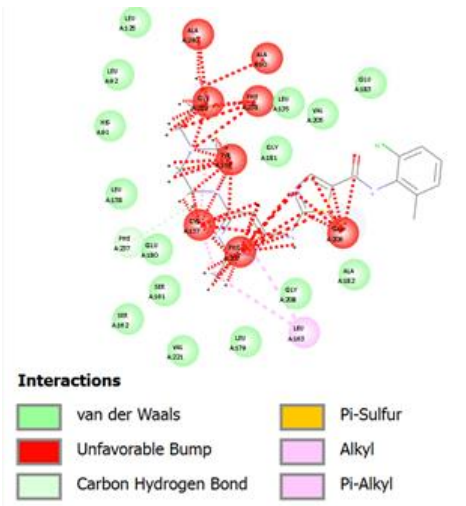

LTB + Dasatinib

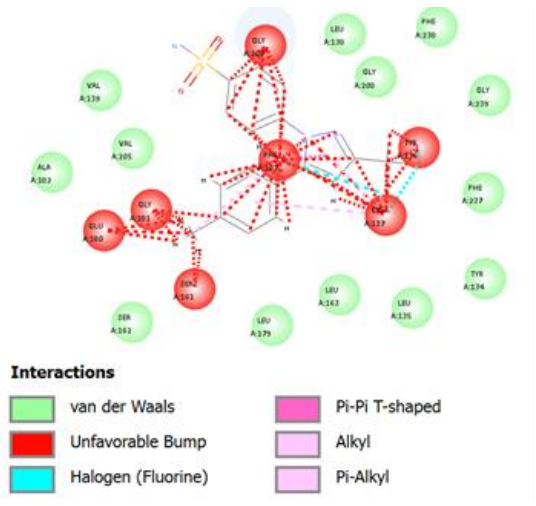

LTB + Celecoxib

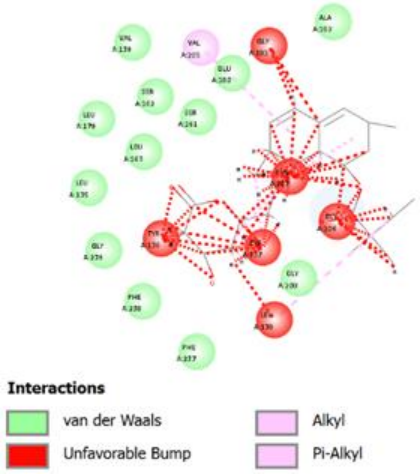

LTB + Simvastatin

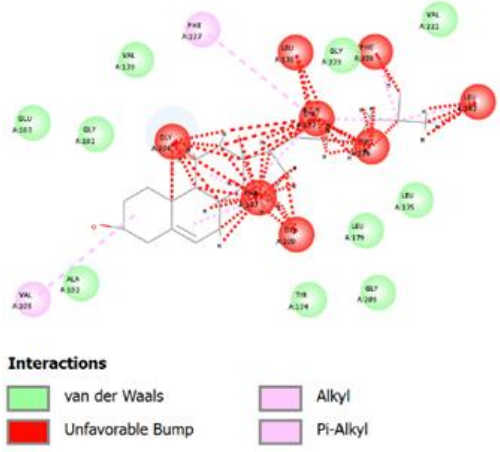

LTB + Cholesterol

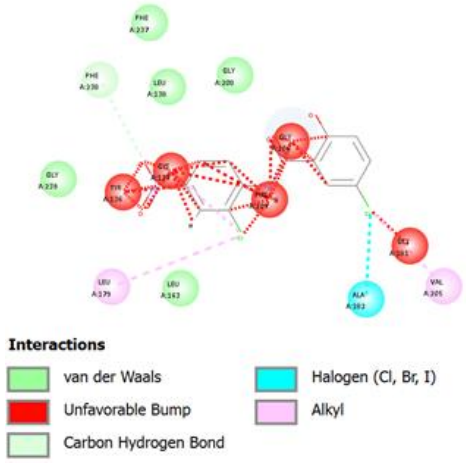

LTB + Niclosamide

Fig. 9. Hydrophilic and Hydrophobic Interactions in LTB–Ligand Complexes Predicted Using Discovery Studio.

DISCUSSION

POEMS syndrome is a rare and complex paraneoplastic disorder characterized by multisystem involvement resulting from an underlying plasma cell dyscrasia. Although clinical recognition of the syndrome has improved in recent years, the molecular mechanisms driving disease onset, progression, and systemic manifestations remain poorly defined (Haider *et al.*, 2023). The present study was undertaken to address this gap by applying a comprehensive *in silico* approach to investigate the molecular landscape of POEMS syndrome, with a particular focus on EHD1, STAT3, KLHL6, and LTB that have been repeatedly implicated in recent genetic and signaling studies. By integrating protein–protein interaction (PPI) network analysis, functional gene–gene interaction mapping, homology-based structural modeling, and molecular docking with FDA-approved compounds, this study provides a systems-level perspective on the molecular processes contributing to POEMS syndrome. Such an approach is especially valuable for rare disorders, where experimental data and patient-derived samples are limited.

Protein–protein interaction analysis demonstrated that EHD1 occupies a central position within a tightly interconnected network enriched for proteins involved in vesicular trafficking, endocytic recycling, and membrane dynamics, including RAB11A, RAB5A, ARF6, SNX27, MICALL1, and members of the RAB11FIP family. These findings are consistent with the established role of EHD1 in regulating endosomal transport and receptor recycling. In the POEMS syndrome, dysregulated cytokine signaling represents a key pathological feature, and endocytic recycling pathways are critical in controlling the intensity and duration of cytokine receptor signaling by modulating receptor internalization and re-presentation at the cell surface. Aberrant EHD1 activity may therefore prolong cytokine receptor availability on the plasma membrane, resulting in sustained downstream signaling and excessive cytokine production. This mechanism may contribute indirectly to elevated VEGF levels and the vascular permeability, edema, and organomegaly that characterize POEMS syndrome (Bou Zerdan *et al.*, 2022; Lapietra *et al.*, 2021).

Moreover, STAT3 showed the most extensive interaction network, connecting with JAK1, JAK2, JAK3, EGFR, SRC, PIAS3, EP300, and other STAT family proteins. This reflects its central role in regulating inflammatory, proliferative, and survival pathways. In POEMS syndrome, STAT3 likely contributes to increased expression of VEGF, IL-6, and other pro-angiogenic and inflammatory mediators. Its interactions with proteins such as EP300 suggest a role in transcriptional regulation that supports abnormal plasma cell survival, highlighting STAT3 as a potential target for therapy (Kundu *et al.*, 2024; Tomasso *et al.*, 2022). KLHL6 exhibited a smaller interaction network, with partners such as GLUL, GLUD1, CTBP2, COPS8, and GPRL1, indicating roles in metabolism, protein stability, and cellular homeostasis. As a BTB–Kelch adaptor, KLHL6 may regulate substrates via ubiquitination. Recurrent mutations in POEMS syndrome suggest disrupted B-cell signaling and plasma cell differentiation, contributing to clonal expansion and altered metabolism that may drive disease progression.(Kroll *et al.*, 2005; Meriranta *et al.*, 2024).

The LTB-centered interaction network was enriched for immune-related proteins, including LTA, TNFRSF13C, TNFRSF1B, CD40LG, TRAF3, and RELB, underscoring its role in TNF and NF-κB signaling pathways. LTB plays a critical role in lymphoid tissue organization and immune cell communication, and its dysregulation may contribute to the immune activation and inflammatory features frequently observed in POEMS syndrome, including its association with Castleman disease (Chen *et al.*, 2024). Structural modeling of EHD1, STAT3, KLHL6, and LTB using SWISS-MODEL produced reliable three-dimensional protein structures, as confirmed by PROCHECK, VERIFY3D, and ERRAT validation analyses. The majority of residues were located in the most favored regions of the Ramachandran plots, indicating acceptable stereochemical quality and suitability for molecular docking

studies. Our study identified several FDA-approved compounds, Dasatinib, Simvastatin, Celecoxib, Niclosamide, Acitretin, and Cholesterol, with strong predicted docking scores across multiple target proteins. The docking analysis revealed that all ligands formed multiple hydrophilic and hydrophobic interactions with key residues of their target proteins, stabilizing binding within functional regions. EHD1 ligands engaged residues such as ASN288, SER284, VAL61, ILE214, and ARG215, while STAT3 ligands interacted with ARG350, CYS259, PRO256, LYS244, and TRP243. KLHL6 ligands formed contacts with residues including TYR297, GLU307, ARG515, LEU343, and CYS556, and LTB ligands bound hydrophilically and hydrophobically to residues such as GLU180, SER161, LEU125, PHE237, and VAL221. These interactions indicate strong ligand stabilization and potential modulation of protein function.

Notably, Dasatinib demonstrated consistent binding to STAT3, KLHL6, and LTB. As a tyrosine kinase inhibitor with known immunomodulatory effects, Dasatinib may suppress cytokine-driven signaling pathways, including those mediated by STAT3, thereby potentially reducing VEGF-driven angiogenesis and inflammation. Simvastatin and Celecoxib also exhibited favorable interactions with multiple targets, including EHD1, KLHL6, and STAT3. Statins are known to exert pleiotropic anti-inflammatory effects beyond lipid-lowering, while Celecoxib inhibits COX-2-mediated inflammatory pathways. Their predicted binding profiles suggest potential repurposing opportunities for modulating disease-relevant pathways in POEMS syndrome. Niclosamide, which has been reported to inhibit STAT3 signaling in other disease contexts, also showed favorable docking interactions with STAT3 and KLHL6, supporting its candidacy for further investigation.

The identification of repurposable FDA-approved compounds represents a practical advantage in rare diseases, where traditional drug development is often challenging. Agents capable of targeting multiple disease-associated pathways may offer improved therapeutic efficacy compared with single-target approaches. However, the findings of this study are based solely on computational predictions and do not account for protein dynamics, post-translational modifications, or cellular context. Docking scores may not directly translate to biological activity, and off-target effects cannot be excluded. Furthermore, only a limited subset of FDA-approved compounds was evaluated, potentially overlooking other molecules with greater therapeutic potential. Future studies should focus on experimental validation of the identified protein–ligand interactions using *in vitro* binding assays, cell-based functional analyses, and *in vivo* disease models. Molecular dynamics simulations and expanded compound screening may further refine these findings and support translational application.

CONCLUSION

In conclusion, this study provides a comprehensive computational analysis of the key molecular players implicated in POEMS syndrome, highlighting their roles in vesicular trafficking, cytokine signaling, immune regulation, and plasma cell stability. Detailed interaction network analyses revealed that EHD1 is primarily involved in endocytic recycling and vesicular transport, STAT3 serves as a central mediator of cytokine-dependent transcription, KLHL6 regulates B-cell receptor signaling and plasma cell differentiation, and LTB modulates immune and inflammatory pathways. Homology modeling and structural validation confirmed the reliability of the predicted three-dimensional protein structures, enabling accurate molecular docking studies. Several FDA-approved compounds, including Dasatinib, Simvastatin, Celecoxib, Niclosamide, Acitretin, and Cholesterol, demonstrated favorable binding affinities with one or more of these target proteins, suggesting potential multi-target therapeutic applications. These findings not only offer insights into the structural and functional characteristics of the proteins associated with POEMS syndrome but also provide a framework for the rational selection of candidate drugs for repurposing. Collectively, the results enhance

our molecular understanding of POEMS syndrome, illustrating how dysregulated signaling pathways, immune modulation, and plasma cell abnormalities contribute to disease pathogenesis, and they lay a solid foundation for future translational studies aimed at developing targeted interventions and improving clinical outcomes.

ACKNOWLEDGEMENT

The authors acknowledge the use of publicly available databases and computational tools.

CONFLICT OF INTEREST

The authors declare that they have no conflict of interest.

REFERENCES

Bertocci, B., Lecoeuche, D., Sterlin, D., Kühn, J., Gaillard, B., De Smet, A., Lembo, F., Bole-Feysot, C., Cagnard, N., Fadeev, T., Dahan, A., Weill, J.C., Reynaud, C.A., 2017. Klhl6 Deficiency Impairs Transitional B Cell Survival and Differentiation. J. Immunol., (Baltimore, Md.: 1950), 199(7): 2408-2420.

Bilal, I., Munir, H., Ramzan, K., Zulfiqar, I., Waheed, A., Haider, A., Ali, F., 2025a. Structural modeling and functional prediction of ifn-y gene variants. Quantum J. Med. Health Sci., 4(3): 84-102.

Bilal, I., Ramzan, K., Ramzan, S., Zulfiqar, M., Tahir, U., Moazzam, A., Haider, I., 2025b. Homology Modeling and Structural Docking Analysis on a Human BDNF Gene by Using Computational Algorithms. J. Adv. Biol. Biotechnol., 28(4): 464–487.

Bou Zerdan, M., George, T.I., Bunting, S.T., Chaulagain, C.P., 2022. Recent Advances in the Treatment and Supportive Care of POEMS Syndrome. J. Clin. Med., 11(23): 7011.

Chakrabarti, R., Lee, M., Higgs, H.N., 2021. Multiple roles for actin in secretory and endocytic pathways. Curr. Biol., 31(10): R603-R618.

Chen, J., Gao, X.M., Zhao, H., Cai, H., Zhang, L., Cao, X.X., Zhou, D.B., Li, J., 2021. A highly heterogeneous mutational pattern in POEMS syndrome. Leukemia, 35(4): 1100-1107.

Chen, Q., Muñoz, A.R., Korchagina, A.A., Shou, Y., Vallecer, J., Todd, A.W., Shein, S.A., Tumanov, A.V., Koroleva, E., 2024. LTβR-RelB signaling in intestinal epithelial cells protects from chemotherapy-induced mucosal damage. Front. Immunol., 15: 1388496.

Dhanoa, B., Cogliati, T., Satish, A., Bruford, E., Friedman, J., 2013. Update on the Kelch-like (KLHL) gene family. Human Genom., 7: 13.

Dispenzieri, A., 2021. POEMS syndrome: 2021 Update on diagnosis, risk-stratification, and management. Am. J. Hematol., 96(7): 872-888.

Dispenzieri, A., Buadi, F., 2013. A review of POEMS syndrome. Oncology (Williston Park, N.Y.), 27: 1242-50.

Haider, S.A., Iram, S., Rashid, A.A., Manazar, A., Javed, H., 2023. POEMS (Polyneuropathy, Organomegaly, Endocrinopathy, Monoclonal Plasma Cell Disorder, and Skin Changes) Syndrome as a Sequela of Castleman Disease: A Case Report. Cureus., 15(11): e49330.

Jones, T., Naslavsky, N., Caplan, S., 2020. Eps15 Homology Domain Protein 4 (EHD4) is required for Eps15 Homology Domain Protein 1 (EHD1)-mediated endosomal recruitment and fission. PloS One., 15(9): e0239657.

Kim, Y.R., 2022. Update on the POEMS syndrome. Blood Res., 57(S1): 27-31.

Kroll, J., Shi, X., Caprioli, A., Liu, H.H., Waskow, C., Lin, K.M., Miyazaki, T., Rodewald, H.R., Sato, T.N., 2005. The BTB-kelch protein KLHL6 is involved in B-lymphocyte antigen receptor signaling and germinal center formation. Mol. Cell. Biol., 25(19): 8531-40.

Kuchipudi, S., 2015. The complex role of STAT3 in viral infections. J. Immunol. Res., 2015: 1-9.

Kundu, G., Ghasemi, M., Yim, S., Rohil, A., Xin, C., Ren, L., Srivastava, S., Akinfolarin, A.,

Kumar, S., Srivastava, G.P., Sabbisetti, V.S., Murugaiyan, G., Ajay, A.K., 2024. STAT3 Protein-Protein Interaction Analysis Finds P300 as a Regulator of STAT3 and Histone 3 Lysine 27 Acetylation in Pericytes. Biomed., 12(9).

Lapietra, G., Fazio, F., Petrucci, M.T., 2021. The unclear role of VEGF in POEMS syndrome: therapeutic implications of neoangiogenesis in a rare plasma cell disorder. J. Cancer Metastasis Treat., 7: 61.

Liu, Y., Yang, X., Gan, J., Chen, S., Xiao, Z.X., Cao, Y., 2022. CB-Dock2: improved protein-ligand blind docking by integrating cavity detection, docking and homologous template fitting. Nucleic Acids Res., 50(W1): W159-w164.

Meriranta, L., Sorri, S., Huse, K., Liu, X., Spasevska, I., Zafar, S., Chowdhury, I., Dufva, O., Sahlberg, E., Tandarić, L., Karjalainen-Lindsberg, M.L., Hyytiäinen, M., Varjosalo, M., Myklebust, J.H., Leppä, S., 2024. Disruption of KLHL6 Fuels Oncogenic Antigen Receptor Signaling in B-Cell Lymphoma. Blood Cancer Discov., 5(5): 331-352.

Nagao, Y., Mimura, N., Takeda, J., et al., 2019. Genetic and transcriptional landscape of plasma cells in POEMS syndrome. Leukemia, 33(7): 1723-1735.

Noman, A., Sardar, N., Islam, A., Ramzan, K., Ali, M.Z., Tahir, H.U., Waheed, A., Parveen, M., 2025. Integrative Computational Analysis of CFTR Mutations Linked to Cystic Fibrosis. Int. J. Mol. Microbiol., 8(1): 52-69.

Nozza, A., 2017. POEMS SYNDROME: an Update. Mediterr. J. Hematol. Infect. Dis., 9(1): e2017051.

Ramzan, K., Noman, A., 2024. Structural Analysis And Protein-Ligand Docking Approach Of BrainAssociated APOE, SNCA, And PRKN Genes. Int. J. Pharm. Sci., 2: 393-410.

Rasheed, A., Safdar, M., Umar, A., Khan, M.S., Ramzan, S., Ramzan, K., Sabri, S., Shaffique, S., Tahir, M.Z., 2025. Comparative bioinformatics analysis and functional characteristics of natriuretic peptide B (NPPB) gene in humans. In Silico Res. Biomed., 1: 100074.

Samad, M.A., Ahmad, I., Hasan, A., Alhashmi, M.H., Ayub, A., Al-Abbasi, F.A., Kumer, A., Tabrez, S., 2025. STAT3 Signaling Pathway in Health and Disease. MedComm, 6(4): e70152.

Sardar, N., Noman, A., Ramzan, K., Bilal, I., Islam, A., Ali, M.Z., Tahir, H.U., Akram, N., Siddique, A.H., Usman, M., 2025. Exploring the Impact of STAT4 Non-Synonymous Mutations on Hepatitis B Virus Susceptibility: A Bioinformatics Approach. Int. J. Mol. Microbiol., 8(1): 79-102.

Suichi, T., Misawa, S., Sato, Y., Beppu, M., Sakaida, E., Sekiguchi, Y., Shibuya, K., Watanabe, K., Amino, H., Kuwabara, S., 2018. Proposal of new clinical diagnostic criteria for POEMS syndrome. J. Neurol. Neurosurg. Psychiatr., 90: jnnp-2018.

Tomasso, A., Innocenti, I., Autore, F., Fresa, A., Benintende, G., Vuono, F., Baroni, S., Giannotta, C., Chiusolo, P., Sorà, F., Sica, S., Laurenti, L., 2022. VEGF and IL-6 Correlation in POEMS: a Potential Upcoming Marker of Active Disease and Early Autologous BMT Response. Mediterr. J. Hematol. Infect. Dis., 14(1): e2022007.

Upadhyay, V., Fu, Y.X., 2013. Lymphotoxin signalling in immune homeostasis and the control of microorganisms. Nat. Rev. Immunol., 13(4): 270-9.

Upadhyay, V., Fu, Y.X., 2014. Lymphotoxin organizes contributions to host defense and metabolic illness from innate lymphoid cells. Cytokine Growth Factor Rev., 25(2): 227-33.

Watanabe, O., Arimura, K., Kitajima, I., Osame, M., Maruyama, I., 1996. Greatly raised vascular endothelial growth factor (VEGF) in POEMS syndrome. Lancet (London, England), 347(9002): 702.